Title	Screen printed epidermal antenna for IoT health monitoring
Author(s)	Simorangkir, Roy B. V. B.; Gawade, Dinesh R.; Kumar, Sanjeev; O'Flynn, Brendan; Buckley, John; Hannon, Tim; Donovan, Paul; Newberry, Robert
Publication date	2022-01-03
Original citation	Simorangkir, R. B. V. B., Gawade, D. R., Kumar, S., O'Flynn, B., Buckley, J. L., Hannon, T., Donovan, P. and Newberry, R. (2021) 'Screen printed epidermal antenna for IoT health monitoring', 2021 IEEE Asia-Pacific Microwave Conference (APMC), Brisbane, Australia, 28 November-01 December, pp. 395-397. doi: 10.1109/APMC52720.2021.9661904
Type of publication	Conference item
Link to publisher's version	http://dx.doi.org/10.1109/APMC52720.2021.9661904 Access to the full text of the published version may require a subscription.
Rights	**© 2021 IEEE. Personal use of this material is permitted. Permission from IEEE must be obtained for all other uses, in any current or future media, including reprinting/republishing this material for advertising or promotional purposes, creating new collective works, for resale or redistribution to servers or lists, or reuse of any copyrighted component of this work in other works**
Item downloaded from	http://hdl.handle.net/10468/12565

Screen Printed Epidermal Antenna for IoT Health Monitoring

Roy B. V. B. Simorangkir, Dinesh R. Gawade,
Sanjeev Kumar, Brendan O'Flynn,
John L. Buckley
Tyndall National Institute, University College Cork
Dyke Parade, T12R5CP Cork, Ireland

Tim Hannon, Paul Donovan
Robert Newberry
Sanmina Corporation
13000 S. Memorial Parkway
Huntsville, AL 35803, USA

***Abstract*—In this paper, we investigate the applicability of screen printable elastic silver ink on thermoplastic polyurethane (TPU) substrate for the realization of a flexible/stretchable antenna for direct implementation on human skin. For this purpose, we present the design, manufacture, and testing of an ultra-high frequency (UHF) 868 MHz loop antenna with the specified material. The antenna performance has been investigated through simulations and measurements on a human forearm phantom, including indoor wireless communication tests, demonstrating its potential for short-range IoT health monitoring applications.**

***Index Terms*—Epidermal antennas, flexible antennas, screen printing, silver ink, stretchable antennas.**

I. Introduction

Epidermal electronics is a class of ultrathin and lightweight electronic systems, which can noninvasively be mounted onto the surface of the human skin [1]. In recent years, epidermal electronics has emerged as a promising technology that enables seamless monitoring of human physiological parameters and wellness [2]. Epidermal antennas are one of the key enabling technologies required for epidermal electronics so as to enable wireless communication capability for the monitoring system with entities either inside or outside the body, or for enabling self-powering of the system through electromagnetic energy harvesting [3]–[5].

Epidermal antennas are desired to be flexible, stretchable, bio compatible, water resistant, and lightweight so as to enable a seamless and intimate integration to skin. To achieve this, epidermal antennas are typically developed using ultrathin and flexible materials. Polymer-based flexible materials, such as polydimethylsyloxane (PDMS) [3], bio-silicone [6], and hydrogels [7], are some popularly used substrate materials for epidermal antennas. However, employing these flexible/stretchable materials to develop epidermal antennas with characteristics suitable for epidermal applications often requires a complex manufacturing process involving multiple-steps high-temperature vacuum deposition, photolithographic patterning, and chemical etching [8]. As a result, inherently flexible/stretchable conductive and non-conductive materials that are compatible with printing technologies such as screen and inkjet printing have attracted the attention of the research community as they allow for a simplified design process and lower cost of production. In this paper, we demonstrate the screen printing of elastic silver ink on a stretchable thermoplastic polyurethane (TPU) substrate for the development of epidermal antennas suitable for epidermal IoT health monitoring applications.

II. Antenna Design and Prototype

The proposed antenna used for this study is shown in Fig. 1(a), which is a modification of a rectangular loop antenna, with a ground plane on one of its sides to achieve better control of impedance matching. The antenna was designed at the European long-range wide area network (LoRaWAN) frequency band, i.e., 863–870 MHz [9], [10], using the full-wave electromagnetic (EM) simulator ANSYS HFSS [11]. In the simulation, a forearm phantom was taken into account as depicted in Fig. 1(b) to emulate the envisaged wireless sensing application employed on a human arm. The phantom consists of a double-layer cylinder following the structure of SHO-GFPC-V1 forearm phantom from SPEAG [12] used in the antenna measurement. The forearm tissue was modeled with ε_r = 30 and σ = 0.7 S/m, whereas the forearm bone was modeled with ε_r = 30 and σ = 2.5 S/m, following the averaged electrical properties of the forearm at 868 MHz according to the SPEAG phantom datasheet [12].

It was observed in the simulation that the antenna gain is primarily governed by the antenna aperture ($s1$ and $s2$), whereas the antenna impedance matching is controlled by the width of the loop and ground (w and g). In contrast to a loop antenna in free space, however, as the antenna aperture is increased, the radiation performance improves at first, then peaks, before decreasing somewhat or remaining rather steady, displaying a bell-shaped pattern. A similar occurrence was recently reported in [13], suggesting that the cause being two opposing phenomena, i.e., the antenna radiation resistance and the power dissipation. This can be explained in the following way. The initial increase in antenna radiation is mostly due to an increase in the radiation resistance, which is proportional to the loop aperture size [14]. Further enlargement of the antenna size however, results in more intense dissipation of power in the antenna conductors and the surrounding phantom, which is also a conductive substance. This causes the amplitude of the currents flowing through the conductor to gradually decrease, resulting in an inefficient utilization of the available conductive

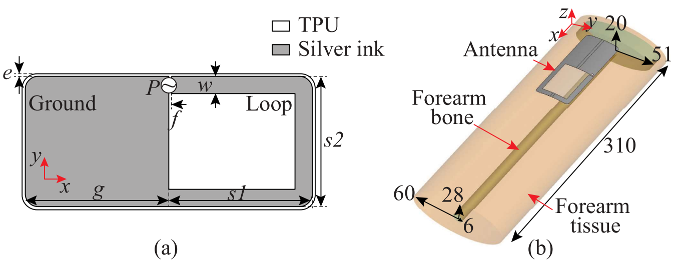

Fig. 1. (a) Topology of the proposed antenna (Dimensions: $s1$ = 50, $s2$ = 51, g = 50, w = 6, f = 1, e = 1.) (b) EM simulated model of the antenna placed on a forearm phantom. All units in the figure are in millimeters.

surface and therefore affecting antenna radiation efficiency and gain.

For the antenna conductive structure, elastic screen printable silver ink, WIK21285-89A, from Henkel [15] was used, which was modeled as a 10 μm thick metal with a conductivity of 3.94×10^6 S/m according to the datasheet. A seam tape ST604 from Bemis [16] was used as the substrate. ST604 is made of TPU material which has a total thickness of 89 μm. It also comes with a carrier layer with a thickness of 137 μm to support the TPU during drying. The TPU substrate was modeled in simulation with ε_r = 4.18 and tan δ = 0.075, obtained from measurements conducted at 868 MHz using a Dielectric Assessment Kit, DAK3.5-TL, from SPEAG [17]. The antenna prototype was screen printed over the TPU substrate with a polyester mesh screen (300M), and then dried in an oven at a temperature of 120° for a duration of 15 min according to the recommendation provided in the ink datasheet [15]. Upon drying, the carrier layer was detached from the substrate. The fabricated prototype is shown in Fig. 2. For measurement purposes, a U. FL connector and U. FL-to-SMA cable are used at the feed point. The connector was attached to the antenna using a conductive silver epoxy. To strengthen the connection, a non-conductive glue was applied, covering the U. FL and cable interconnection.

III. Antenna Performance

The measured input reflection coefficient ($|S_{11}|$) of the antenna mounted on top of the SPEAG forearm phantom is shown in Fig. 3(a), which was obtained using a MS2038C Vector Network Analyzer (VNA) from Anritsu. A ferrite bead was incorporated in the measurement setup to minimize ground current flow on the feed cable that can perturb the measured impedance and radiation characteristics of the antenna. The antenna exhibits a 10-dB return loss bandwidth of more than 2 GHz, showing a good agreement with the simulated result. Discrepancies in the results are most likely due to the antenna fabrication tolerances and the morphology variation between the model and the actual phantom. The simulated 3D radiation pattern of the antenna on the phantom at 868 MHz is shown in Fig. 3(b), showing a peak realized gain of -18.1 dBi, which is within the typical performance range of a loop antenna in a very close proximity to the lossy human body tissue [13].

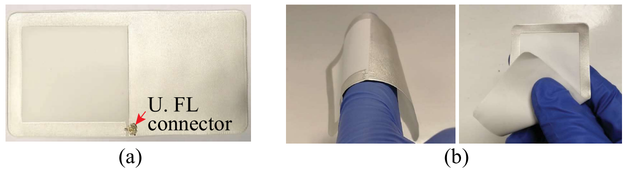

Fig. 2. (a) Screen-printed antenna prototype upon U. FL connector assembly. (b) Antenna under deformation demonstrating its flexibility.

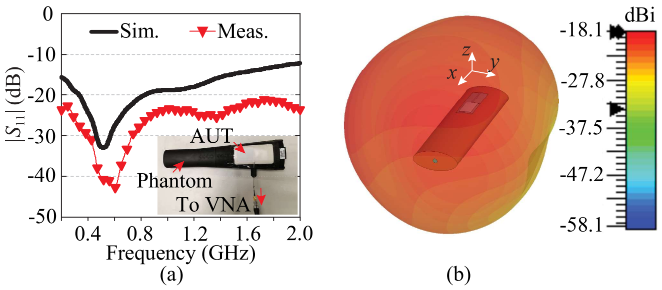

Fig. 3. (a) Measured and simulated $|S_{11}|$ when the antenna attached on the phantom as illustrated in the inset. (b) Simulated 3D radiation pattern of the antenna at 868 MHz.

IV. Indoor Wireless Communication Test

To demonstrate the applicability of the developed antenna for IoT health monitoring applications, a simple LoRaWAN testbed network, consisting of one node and one gateway, was deployed inside the Tyndall National Institute building (Block A) (Fig. 4(a)). For the gateway, a commercial LoRa gateway (TTN-GW-868) [18] shown in Fig. 4(b) was used. The node comprises of a commercial LoRa module (L072Z-LRWAN1) [19] connected to a temperature and humidity expansion board (X-NUCLEO-IKS01A2) [20] and the developed epidermal antenna mounted on the SPEAG phantom (Fig. 4(c)). The node (N) transmitted measured temperature and relative humidity data to the gateway (G) with an adaptive spreading factor (SF) setting of 7 to 12. The gateway was connected to the LoRaWAN network server of The Things Network (TTN), which was responsible for the network and data management, as well as some other operations such as filtering redundant received packets, performing security checks and adaptive data rate (ADR) changes, as well as forwarding data packets to the user data portal for visualization and storing.

The node was then moved to three different locations inside the building, i.e., N_1, N_2, and N_3 (Fig. 4), and Received Signal Strength Indicator (RSSI) values were recorded for each location. The RSSI metric is a relative power level indicator which in this scenario indicates how well the gateway can receive the signal form the wirelessly connected sensor node. From the tests, RSSI values of -79 dBm, -90 dBm, and -119 dBm were measured when the node was approximately 5 m (N_1), 25 m (N_2), and 30 m (N_3) non-line-of-sight away from the gateway. To note that, a LoRaWAN network can offer a maximum receiver sensitivity of -137 dBm at SF12 [21]. Further, at one of the locations (i.e., N_1), we also monitored over a longer

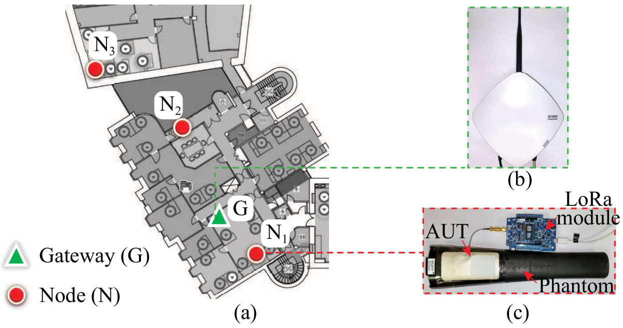

Fig. 4. (a) LoRaWAN testbed network. (b) LoRa Gateway and (c) node used for the indoor wireless communication tests.

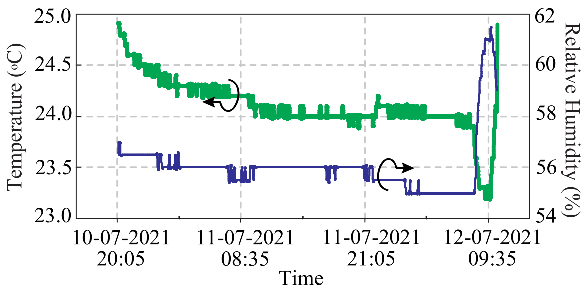

Fig. 5. Measured temperature and humidity results.

period of time the measured temperature and humidity data packets transmitted from the node to the gateway which is shown in Fig. 5. From approximately 38 hours and 15 minutes duration of the test, 100% data packets reception rate was achieved.

V. Conclusion

In this paper, we demonstrated the design, implementation, and testing of a screen printed elastic silver ink over a TPU substrate for epidermal antenna realization. The antenna performance, including the indoor wireless communication tests, demonstrates the applicability of the developed antenna for epidermal IoT applications, such as human health monitoring. Further studies in improving the radiation performance of the antenna as well as a holistic integration with a customized wireless module are planned as a future work.

Acknowledgement

This work was supported in part by the Enterprise Ireland funded HOLISTICS DTIF project (EIDT20180291-A), as well as by Science Foundation Ireland (SFI) under the following Grant Numbers: Connect Centre for Future Networks and Communications (13/RC/2077) and the Insight Centre for Data Analytics (SFI/12/RC/2289), as well as the European Regional Development Fund. The authors would like to thank Henkel, especially Dr Carla Negele, for providing free samples of WIK21285-89A silver ink and ST604 TPU substrate.

References

[1] D.-H. Kim et. al., "Epidermal electronics," *Science*, vol. 333, no. 6044, pp. 838–843, 2011. [Online]. Available: https://science.sciencemag.org/content/333/6044/838

[2] N. Lu, S. K. Ameri, T. Ha, L. Nicolini, A. Stier, and P. Wang, "Epidermal electronic systems for sensing and therapy," in *Nanosensors, Biosensors, Info-Tech Sensors and 3D Systems 2017*, V. K. Varadan, Ed., vol. 10167, International Society for Optics and Photonics. SPIE, 2017, pp. 84 – 90. [Online]. Available: https://doi.org/10.1117/12.2261755

[3] X. Huang et. al., "Epidermal radio frequency electronics for wireless power transfer," *Microsystems and Nanoengineering*, vol. 2, no. 1, p. 16052, 2016.

[4] G. León, L. F. Herrán, I. Mateos, E. Villa, and J. B. Ruiz-Alzola, "Wideband epidermal antenna for medical radiometry," *Sensors*, vol. 20, no. 7, 2020. [Online]. Available: https://www.mdpi.com/1424-8220/20/7/1987

[5] H. A. Damis, N. Khalid, R. Mirzavand, H.-J. Chung, and P. Mousavi, "Investigation of epidermal loop antennas for biotelemetry iot applications," *IEEE Access*, vol. 6, pp. 15 806–15 815, 2018.

[6] S. Amendola, S. Milici, and G. Marrocco, "Performance of epidermal rfid dual-loop tag and on-skin retuning," *IEEE Transactions on Antennas and Propagation*, vol. 63, no. 8, pp. 3672–3680, 2015.

[7] C. Lim, Y. Shin, J. Jung, J. H. Kim, S. Lee, and D.-H. Kim, "Stretchable conductive nanocomposite based on alginate hydrogel and silver nanowires for wearable electronics," *APL Materials*, vol. 7, no. 3, p. 031502, 2019. [Online]. Available: https://doi.org/10.1063/1.5063657

[8] T. Zhong, N. Jin, W. Yuan, C. Zhou, W. Gu, and Z. Cui, "Printable stretchable silver ink and application to printed rfid tags for wearable electronics," *Materials*, vol. 12, no. 18, 2019. [Online]. Available: https://www.mdpi.com/1996-1944/12/18/3036

[9] E. De Poorter et. al., "Sub-GHz LPWAN network coexistence, management and virtualization: an overview and open research challenges," *Wireless Personal Communications*, vol. 95, p. 187–213, 2017.

[10] S. Kumar, J. L. Buckley, J. Barton, M. Pigeon, R. Newberry, M. Rodencal, A. Hajzeraj, T. Hannon, K. Rogers, D. Casey, D. O'Sullivan, and B. O'Flynn, "A wristwatch-based wireless sensor platform for iot health monitoring applications," *Sensors*, vol. 20, no. 6, 2020. [Online]. Available: https://www.mdpi.com/1424-8220/20/6/1675

[11] ANSYS HFSS. Accessed: 25 July 2020. [Online]. Available: http://www.ansys.com/products/electronics/ansys-hfss

[12] Speag Phantom Arm, SHO-GFPC-V1. Accessed: 15 February 2021. [Online]. Available: https://speag.swiss/products/em-phantoms/phantoms/sho-gfpc-v1/

[13] S. Amendola and G. Marrocco, "Optimal performance of epidermal antennas for UHF radio frequency identification and sensing," *IEEE Trans. Antennas Propag.*, vol. 65, no. 2, pp. 473–481, 2017.

[14] C. A. Balanis, "Loop antennas," in *Antenna Theory*, 3rd ed. Hoboken, New Jersey: John Wiley and Sons, Inc., 2005, ch. 5, pp. 272–273.

[15] Inks coating. Accessed: 15 Feb. 2021. [Online]. Available: https://www.henkel-adhesives.com/uk/en.html

[16] ST604 Seam Tape. Accessed: 15 Feb. 2021. [Online]. Available: https://www.bemisworldwide.com

[17] SPEAG Dielectric Assessment Kit: DAK3.5-TL. Accessed: 15 Feb. 2021. [Online]. Available: https://speag.swiss/products/dak/dak-dielectric-probe-systems/dak3-5tlp-200mhz-20ghz/

[18] The Things Gateway. Accessed: 13 July 2021. [Online]. Available: http://www.farnell.com/datasheets/2552236.pdf

[19] STM32L0 Discovery kit LoRa, Sigfox, low-power wireless. Accessed: 13 July 2021. [Online]. Available: https://www.st.com/en/evaluation-tools/b-l072z-lrwan1.html

[20] Motion MEMS and environmental sensor expansion board for STM32 Nucleo. Accessed: 13 July 2021. [Online]. Available: https://www.st.com/en/ecosystems/x-nucleo-iks01a2.html

[21] Semtech, "Understanding the LoRa Adaptive Data Rate," Semtech Corporation, Tech. Rep., 2019. [Online]. Available: https://lora-developers.semtech.com/library/tech-papers-and-guides/understanding-adr/